Acta Crystallographica Section F
Structural Biology and Crystallization Communications
ISSN 1744-3091

Crystallization and preliminary X-ray analysis of the complex of the first von Willebrand type C domain bound to bone morphogenetic protein 2

Li-yan Qiu,[a] Jin-li Zhang,[a] Alexander Kotzsch,[b] Walter Sebald[a,c] and Thomas D. Mueller[b,c]*

[a]Lehrstuhl für Physiologische Chemie II, Theodor-Boveri-Institut (Biozentrum) der Universität Würzburg, Am Hubland, D-97074 Würzburg, Germany, [b]Lehrstuhl für Molekulare Pflanzenphysiologie und Biophysik, Julius-von-Sachs Institut der Universität Würzburg, Julius-von-Sachs Platz 2, D-97082 Würzburg, Germany, and [c]Rudolf-Virchow-Zentrum (DFG Forschungszentrum) der Universität Würzburg, Versbacher Strasse 9, D-97070 Würzburg, Germany.

Correspondence e-mail: mueller@botanik.uni-wuerzburg.de

Received 5 February 2008
Accepted 12 March 2008

Crossveinless 2 (CV2) is a member of the chordin family, a protein superfamily that modulates the activity of bone morphogenetic proteins such as BMP2. The BMPs represent a large group of secreted proteins that control many steps during embryonal development and in tissue and organ homeostasis in the adult organism. The gene encoding the first von Willebrand type C domain (VWC1) of CV2 was cloned, expressed in *Escherichia coli* and purified to homogeneity. The binary complex of CV2 VWC1 and BMP2 was purified and subjected to crystallization. Crystals of SeMet-labelled proteins were obtained in two different forms belonging to the tetragonal space groups $P4_12_12$ and $I4_1$, with unit-cell parameters $a = b = 86.7$, $c = 139.2$ Å and $a = b = 83.7$, $c = 139.6$ Å, respectively. Initial analysis suggests that a complete binary complex consisting of one BMP2 dimer bound to two CV2 VWC1 domains is present in the asymmetric unit.

1. Introduction

The bone morphogenetic proteins (BMPs) belong to the large TGF-β superfamily of secreted signalling proteins that play important roles during embryonal development (Hogan, 1996; Kondo, 2007) and in tissue homeostasis in the adult organism (for examples, see Li & Cao, 2006; Simic & Vukicevic, 2005). Their manifold functions are tightly controlled, positively and negatively, by extracellular and intracellular inhibitors and modulator proteins (Gazzerro & Canalis, 2006). Extracellular modulators can be separated into membrane-anchored BMP co-receptors, such as BAMBI (Onichtchouk *et al.*, 1999) or DRAGON (Samad *et al.*, 2005), and secreted BMP modulator proteins, such as noggin, follistatin or gremlin. The former can either enhance signalling *via* increased recruitment of BMP ligands to the membrane surface or inhibit BMP activity by competing with BMP receptors, while the latter inactivate BMPs by blocking the BMP–receptor interaction. Modulator proteins of the chordin family present a unique exception to this inhibitory-only function in that they exhibit two contrary activities (Larrain *et al.*, 2001). Depending on the cellular context, chordin and another family member, crossveinless 2 (CV2), can either down-regulate BMP signalling (anti-BMP activity) or enhance BMP signalling (pro-BMP activity) (Binnerts *et al.*, 2004; Ikeya *et al.*, 2006; Rentzsch *et al.*, 2006). The molecular mechanism of this switch in the regulatory mechanism is so far unknown. Both modulator proteins interact with BMPs *via* von Willebrand type C domains, which are present as several copies (Larrain *et al.*, 2000; Zhang *et al.*, 2007). Truncation studies show that only the first VWC domain of CV2 determines binding to BMP2 (Zhang *et al.*, 2007). To date, only structures of BMP2 in its unbound form (Scheufler *et al.*, 1999) and in complexes with its BMP type IA, activin type IIB and activin type II receptors (Allendorph *et al.*, 2006; Kirsch *et al.*, 2000; Weber *et al.*, 2007) are known. However, no structural data are available to date for full-length CV2 or its isolated domains. Thus, determination of the structure of the complex of CV2 VWC1 bound to BMP2 will provide initial insights into how this important class of BMP-modulator proteins interact with members of the TGF-β superfamily. The binding mechanism will allow the

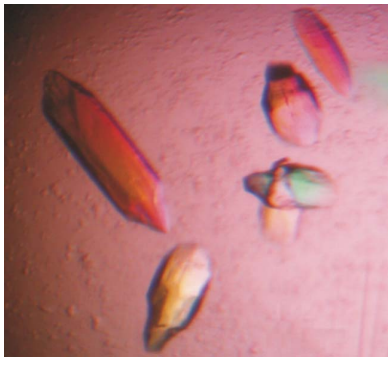

elucidation of how crossveinless 2 and similar chordin-family members uniquely block or enhance the activity of the TGF-β ligands.

2. Materials and methods

2.1. Protein expression and purification

The cDNA encoding residues 1–66 of mature zebrafish CV2 (SWISS-PROT entry Q5D734) was amplified by PCR and cloned into the *Nco*I/*Bpu*1102I sites of a derivative of the expression vector pET32a (Novagen). For protein expression, the expression plasmid pET32a-CV2 VWC1 was transformed into *Escherichia coli* strain Origami B (DE3) (Novagen) host cells. Transformed cells were grown in TB medium at 303 K until the optical density at 600 nm reached about 0.7. The bacterial culture was cooled to 293 K for 30 min and protein expression was subsequently induced by the addition of IPTG (to a final concentration of 1 m*M*) at 293 K for 16 h. After cell lysis, the soluble thioredoxin-CV2 VWC1 fusion protein was first purified using metal-ion affinity chromatography employing Ni^{2+}–NTA resin (Qiagen). The crude cell extract was loaded onto the column in a batch process. The resin was subsequently washed with 150 m*M* NaCl, 10 m*M* Tris pH 7.5 buffer containing 20 m*M* imidazole and the thioredoxin-CV2 VWC1 fusion protein was eluted with 0.5 *M* imidazole. The protein-containing fractions were combined and the protein solution was extensively dialysed against 50 m*M* Tris pH 7.5, 150 m*M* NaCl, 1 m*M* EDTA to remove imidazole. For thrombin cleavage, the protein solution was dialyzed against 50 m*M* Tris pH 7.5, 150 m*M* NaCl, 2.5 m*M* $CaCl_2$ and the thioredoxin-CV2 VWC1 fusion protein was subsequently cleaved using thrombin (10 U per milligram of fusion protein) at 303 K for 3 h. After thrombin cleavage, the CV2 VWC1 protein consisted of residues 1–66 of mature CV2 plus an N-terminal GSW sequence resulting from the expression vector. The CV2 VWC1 protein was separated from thioredoxin employing anion-exchange chromatography using EMD-TMAE Fractogel resin (Merck) and reversed-phase HPLC using a water–acetonitrile gradient in 0.1% trifluoroacetic acid (C4 resin, Vydac). As a final purification step to separate biologically active CV2 VWC1 from inactive protein, affinity chromatography *via* a BMP2-affinity matrix was used. The purity and homogeneity of the CV2 VWC1 protein were assessed by SDS–PAGE, analytical reverse-phase HPLC and ESI FT-ICR mass spectroscopy. BMP2 was expressed in *E. coli* and purified as described in Ruppert *et al.* (1996). Variants of CV2 VWC1 and BMP2 were constructed by PCR using the QuikChange methodology (Stratagene). For the acquisition of a MAD diffraction data set using SeMet derivatives, additional methionine residues were introduced into BMP2 and/or CV2 VWC1 in order to increase the number of methionine residues in the protein complex. For BMP2, a double variant with residues Phe41 and Tyr91 replaced by methionines was used. For CV2 VWC1, which completely lacks methionine, four positions encoding polar amino acids were tested for the introduction of methionines. The four CV2 VWC1 variants with single amino-acid exchanges, *i.e.* S28M, N33M, K39M and E41M, could be expressed and purified in an identical manner to wild-type CV2 VWC1. BIAcore analysis (data not shown) showed that these mutants bind BMP2 with unaltered affinity. Based on these results, the CV2 VWC1 double mutants S28MN33M, N33ME41M and N33MK39M were prepared; however, S28MN33M and N33ME41M variants could not be isolated.

For SeMet labelling, wild-type BMP2, BMP2(Y41M,F91M) and CV2 VWC1(S28M) were prepared by repression of bacterial methionine biosynthesis and complementation of the M9 minimal medium (Van Duyne *et al.*, 1993). To perform this, *E. coli* BL21 (DE3) cells harbouring the plasmids for BMP2, BMP2(Y41M,F91M) or CV2 VWC1(S28M) were grown in M9 minimal medium with glucose (6 g l^{-1}) and ammonium chloride (0.5 g l^{-1}). 20 min prior to induction of protein expression, the medium was supplemented with L-Lys, L-Thr, L-Phe (100 mg l^{-1} each), L-Leu, L-Ile, L-Val (50 mg l^{-1} each) and DL-SeMet (50 mg l^{-1}).

2.2. Crystallization

Since previous experiments had shown that CV2 VWC1 binds to BMP2 with a 2:1 stoichiometry (Zhang *et al.*, 2007), the binary complex of BMP2 and CV2 VWC1 was prepared by mixing BMP2 and CV2 VWC1 in a 1:2.4 molar ratio in 10 m*M* HEPES pH 7.4, 700 m*M* NaCl (HBS_{700} buffer). The complex was then purified by gel filtration in HBS_{700} buffer to remove excess CV2 VWC1 (Figs. 1*a* and 1*b*). The fractions containing the protein complex BMP2–CV2 VWC1 with a 1:2 stoichiometry were combined. The protein complex was concentrated to 8–10 mg ml^{-1} in HBS_{700} buffer and initial crystallization experiments using this protein solution were performed by

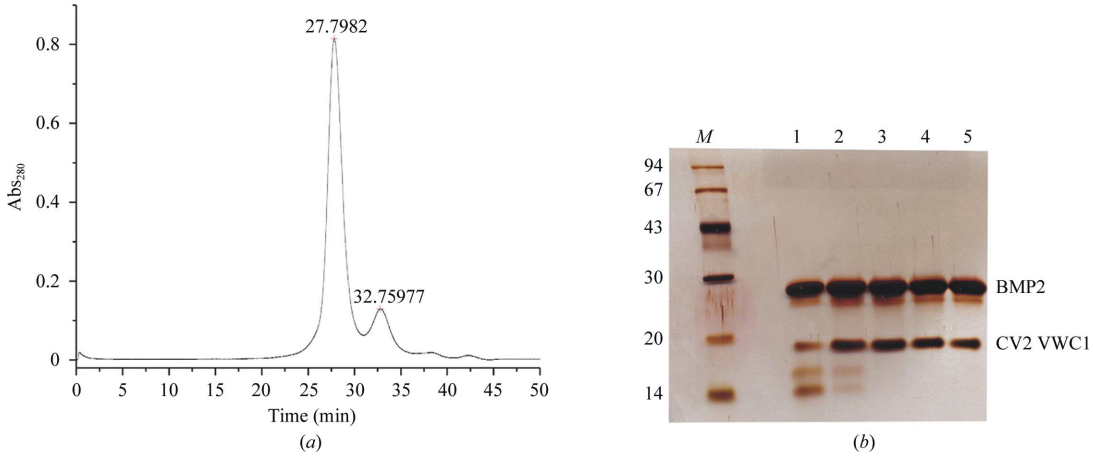

Figure 1
(*a*) Gel filtration of the complex of BMP2 and CV2 VWC1. The peak at 27.79 min corresponds to the binary complex of BMP2 and CV2 VWC1 in a 1:2 stoichiometry. The peak at 32.76 min corresponds to excess CV2 VWC1 separated by the gel filtration. (*b*) SDS–PAGE of individual fractions 1–5 of the gel filtration, showing a stable binary complex of BMP2 bound to CV2 VWC1. Lane *M* contains molecular-weight markers (labelled in kDa). The SDS–PAGE was performed under nonreducing conditions. BMP2 thus migrates as a dimer.

Table 1
Data-collection and processing statistics for the native crystal (BMP2–CV2 VWC1).

Values in parentheses are for the highest resolution shell.

Beamline	PXI, X06SA,SLS
Detector	MAR 225 mosaic
Space group	$P4_1$
Temperature (K)	100
Unit-cell parameters (Å, °)	$a = b = 82.44$, $c = 140.88$, $\alpha = \beta = \gamma = 90$
Wavelength (°)	1.1048
Resolution range (Å)	41.33–3.10 (3.27–3.10)
No. of reflections (total/unique)	126906/17136
Completeness (%)	100.0 (100.0)
Multiplicity	7.4 (7.4)
$R_{\rm merge}$†	0.105 (0.334)
$\langle I/\sigma(I)\rangle$	18.2 (5.7)

† $R_{\rm merge}$ is defined as in Table 2.

sitting-drop vapour-diffusion and sparse-matrix screening at 294 K (Jancarik & Kim, 1991). Each sitting drop was prepared by mixing 1 µl each of protein solution and reservoir solution and was placed over 100 µl reservoir solution. Initial conditions were screened using Hampton Crystal Screens 1 and 2, Index Screen, Lite Screen and Salt Screen kits (Hampton Research, USA). Fine screening was performed employing hanging-drop vapour diffusion and altering the concentrations of the salt and precipitant and the ratio of the protein and precipitant solutions in the hanging drop, as well as the pH of the protein solution used to set up the crystallization trials.

Crystals of the native protein complex BMP2–CV2 VWC1 grew by mixing 1 µl protein complex solution (10 mg ml^{-1}) in HBS_{700} buffer with 1 µl 2.2 *M* ammonium phosphate, 0.1 *M* Tris–HCl pH 7.5, 10%(*w*/*v*) sucrose and placing this mix over reservoir solution consisting of 2.2 *M* ammonium phosphate, 0.1 *M* Tris–HCl pH 7.5, 10%(*w*/*v*) sucrose. Crystals grew to final size within two weeks at 294 K. For crystallization of SeMet derivatives, the complexes SeMet BMP2–SeMet CV2 VWC1(S28M) and SeMet BMP2(Y41M,F91M)–CV2 VWC1 were formed and purified as described above.

SeMet BMP2(Y41M,F91M)–CV2 VWC1 crystals were obtained by mixing 1 µl protein complex (8 mg ml^{-1}) in HBS_{700} buffer with 1 µl 2.0 *M* ammonium phosphate, 0.1 *M* Tris–HCl pH 7.5, 8%(*v*/*v*) glycerol, 5%(*w*/*v*) sucrose and placing the drop over a 1 ml reservoir of the latter solution. Crystals of this complex were slightly smaller and grew within 10 d at 294 K. The second SeMet-labelled complex SeMet BMP2–SeMet CV2 VWC1(S28M) was grown by mixing 1 µl of the protein complex solution (8 mg ml^{-1}) in HBS_{700} buffer with 1 µl 2.2 *M* ammonium phosphate, 0.1 *M* Tris–HCl pH 7.5, 10%(*v*/*v*) glycerol and placing this mixture over a reservoir of the latter solution. Crystals of this SeMet-labelled protein complex grew within 10 d at 294 K.

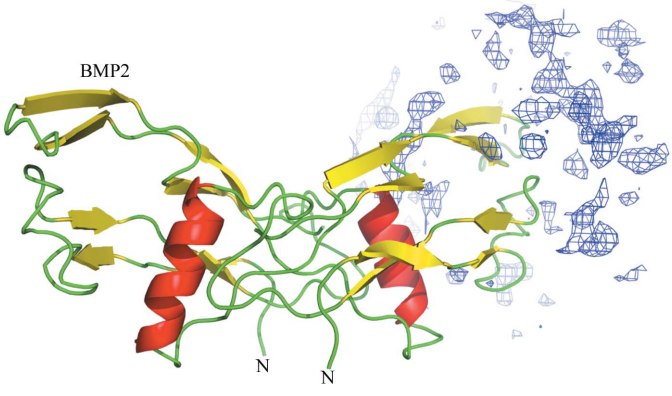

Figure 2
Molecular replacement was initially used to perform phasing of the BMP2–CV2 VWC1 complex. Although two BMP2 dimers could be unambiguously placed in the asymmetric unit (only one is shown), only residual electron density was observed for the CV2 VWC1 molecule at the putative binding site as determined from mutagenesis data (Zhang *et al.*, 2007). One BMP2 dimer is shown in ribbon representation, with part of an $F_{\rm obs} - F_{\rm calc}$ electron-density map contoured at 1.5σ shown around 15 Å of the putative CV2 VWC1-binding site.

2.3. Data collection

A first native diffraction data set was collected from a single crystal of the wild-type BMP2–CV2 VWC1 complex on SLS beamline X06SA (SLS, Villigen, Switzerland). Crystals were mounted in a nylon loop and flash-frozen in liquid nitrogen after soaking the crystals in reservoir solution supplemented with 20% sucrose. The crystal-to-detector distance was set to 250 mm, the wavelength was 1.105 Å and data collection was performed at 100 K. MAD data sets were obtained from SeMet derivatives using crystals of either SeMet BMP2(Y41M,F91M)–CV2 VWC1 or SeMet BMP2–SeMet CV2 VWC1(S28M) on beamline PX14.2 at BESSY (PSF BESSY, Berlin, Germany). Three-wavelength data sets for the two complexes were acquired from single crystals. The crystal-to-detector distance was set to 200 mm. The crystals were rotated through a total of 180°, with 1° oscillation per frame and an exposure time of 5–7 s per frame. Data processing was performed using the software *HKL*-2000 (Otwinowski & Minor, 1997) and *CrystalClear* (Rigaku).

3. Results and discussion

3.1. Crystallization of the wild-type BMP2–CV2 VWC1 complex and preliminary analysis of the native data

Initial crystals of the binary complex of the CV2 VWC1 domain bound to the TGF-β ligand BMP2 were obtained from several crystallization conditions containing salts (ammonium phosphate, ammonium sulfate or malic acid) or polyethylene glycols (molecular-weight range 4000–8000 Da) at pH values varying from slightly acidic to slightly basic. The presence of the complete protein complex was confirmed by harvesting crystals from the initial screening, washing the crystals to remove adhering proteins and analyzing the crystal components *via* SDS–PAGE and silver staining. Screening such crystals for their diffraction capabilities revealed crystals grown from ammonium phosphate to be the most promising for structure analysis. Crystals grown from 2.0–2.2 *M* ammonium phosphate at neutral pH exhibited single-crystal morphology and diffracted to 3–4 Å resolution.

A complete native data set was acquired from a crystal comprising wild-type BMP2 and CV2 VWC1 on beamline X06SA at the SLS (Villigen, Switzerland). The data set from 180 1° frames consists of 17 136 unique reflections. The overall $R_{\rm merge}$ was 10.5% in the resolution range 41.3–3.1 Å and the completeness was 100% (Table 1). The crystal belonged to the tetragonal space group $P4_1$ (or $P4_3$), with unit-cell parameters $a = b = 82.4$, $c = 140.9$ Å. To solve the structure of the complex, molecular replacement was employed using the software *Phaser* (McCoy *et al.*, 2007) with the BMP2 dimer (PDB code 3bmp; Scheufler *et al.*, 1999) as the search template. A clear molecular-replacement solution (LLG = 2292 for both BMP2 dimers, with RFZ = 10.5 and 4.7 and TFZ = 25.0 and 36.2 for the first and second BMP2 molecule, respectively) allowed the placement of two BMP2 dimers in the asymmetric unit and thus confirmed the tetragonal space group $P4_1$ as the correct enantiomer. However, electron density for the CV2 VWC1 domains was vastly incomplete and did not allow

Table 2
Data-collection and processing statistics for SeMet-labelled crystals.

Values in parentheses are for the highest resolution shell.

	SeMet BMP2(Y41M,F91M)–CV2 VWC1			SeMet BMP2–SeMet CV2 VWC1(S28M)		
	Inflection	Peak	Remote	Inflection	Peak	Remote
Beamline	BL14.1,BESSY					
Detector	MAR 225 mosaic					
Space group	$I4_1$			$P4_12_12$		
Temperature (K)	100			100		
Unit-cell parameters (Å, °)	$a = b = 83.70$, $c = 139.63$, $\alpha = \beta = \gamma = 90$			$a = b = 86.71$, $c = 139.19$, $\alpha = \beta = \gamma = 90$		
V_M (Å^3 Da^{-1})	3.32			3.58		
Solvent content (%)	62.7			65.3		
Wilson B factor (Å^2)	57.2			51.1		
Wavelength (Å)	0.9799	0.9796	0.9079	0.9799	0.9796	0.9079
Resolution range (Å)	36.20–2.70 (2.80–2.70)	40.68–2.70 (2.80–2.70)	36.16–2.70 (2.80–2.70)	37.36–3.00 (3.11–3.00)	41.39–3.00 (3.11–3.00)	33.90–3.00 (3.11–3.00)
No. of reflections (total/unique)	43616/13191	43563/13146	43969/13165	59992/11181	60048/11176	39023/9668
Completeness (%)	99.7 (99.7)	99.7 (99.8)	99.7 (100.0)	100.0 (100.0)	99.9 (100.0)	86.4 (90.6)
Multiplicity	3.31 (3.23)	3.31 (3.27)	3.34 (3.27)	5.37 (5.51)	5.37 (5.50)	4.04 (3.97)
R_{merge}†	0.090 (0.342)	0.100 (0.342)	0.099 (0.381)	0.086 (0.311)	0.094 (0.312)	0.099 (0.350)
R_{anom}‡	0.059	0.074	0.071	0.043	0.067	0.069
$\langle I/\sigma(I)\rangle$	8.9 (3.3)	7.7 (3.1)	8.0 (2.7)	11.0 (4.4)	9.9 (4.5)	9.0 (3.5)
Phasing	7 out of 8 Se sites identified, two-wavelength MAD (*SHARP*)			6 out of 6 Se sites identified, three-wavelength MAD (*SHARP*)		
R_{cullis}	0.84	0.72	0.84	0.83	0.71	0.83
R.m.s. lack of closure	0.76	0.92	0.75	0.86	0.93	0.82
Phasing power	1.01	1.38	1.09	1.18	1.41	1.13
Mean figure of merit	0.57			0.57		
Figure of merit after DM	0.74			0.81		

† $R_{merge} = \sum_{hkl}\sum_i |I_i(hkl) - \langle I(hkl)\rangle| / \sum_{hkl}\sum_i I_i(hkl)$, where $I_i(hkl)$ is the intensity of the ith observation of the unique reflection hkl, $\langle I(hkl)\rangle$ being the mean of the intensities of all observations of reflection hkl. ‡ $R_{anom} = \sum_{hkl}(\langle I^+\rangle - \langle I^-\rangle)/\sum_{hkl}(\langle I^+\rangle + \langle I^-\rangle)$.

the building of a model of the full complex (Fig. 2). Using the NMR structures of a distantly related VWC domain of procollagen IIA (PDB code 1u5m; O'Leary *et al.*, 2004) as an additional search template was unsuccessful.

Table 3
Comparison of R_{merge} values for the three data sets.

Values in parentheses are for the highest resolution shell. All R_{merge} values were obtained for the same resolution range of the peak data set and native data set. The respective resolution ranges are shown in Tables 1 and 2. The values in bold designate the data used for structure solution. R_{merge} is defined as in Table 2.

	$I4_1$	$P4_1$	$P4_12_12$
SeMet BMP2(Y41M,F91M)–CV2 VWC1	**0.10 (0.342)**	†	†
SeMet BMP2–SeMet CV2 VWC1(S28M)	†	0.111 (0.364)	**0.094 (0.312)**
BMP2–CV2 VWC1	†	**0.096 (0.383)**	0.267 (0.526)

† Indexing not possible in this space group.

3.2. Crystallization of the SeMet-labelled complexes of BMP2–CV2 VWC1

The SeMet-driven MAD approach was therefore applied for experimental phasing. Since the number of native methionine residues was rather low when using the wild-type proteins (four methionines per BMP2 dimer and none in CV2 VWC1), several residues in BMP2 and CV2 VWC1 were substituted in order to increase the number of methionines. In BMP2 the substitutions

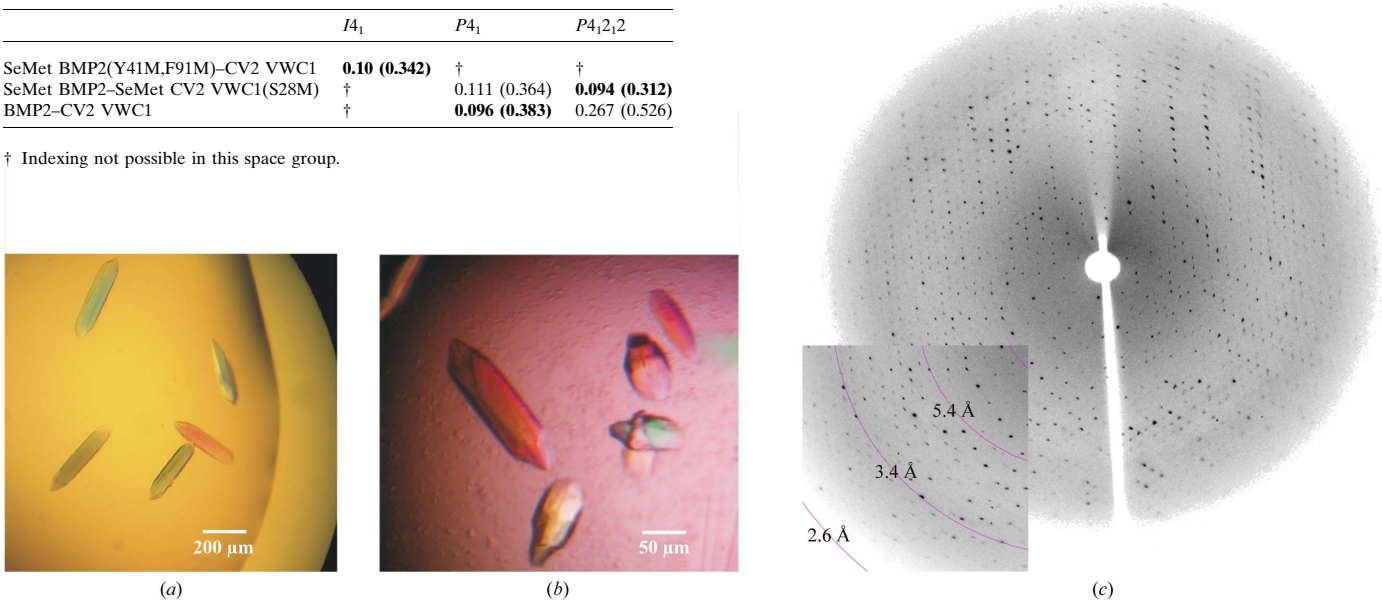

(*a*) (*b*) (*c*)

Figure 3
(*a*) Crystals of the SeMet BMP2(F41M,Y91M)–CV2 VWC1 complex. The crystals grew from 2.0 *M* ammonium phosphate, 0.1 *M* Tris–HCl pH 7.5, 8%(*v*/*v*) glycerol, 5%(*w*/*v*) sucrose and reached dimensions of approximately 0.2 × 0.05 × 0.05 mm. (*b*) Crystals of the complex SeMet BMP2–CV2 VWC1(S28M) grew from 2.2 *M* ammonium phosphate, 0.1 *M* Tris–HCl pH 7.5, 10%(*v*/*v*) glycerol. The dimensions of these crystals were typically 0.2 × 0.05 × 0.05 mm. (*c*) Diffraction pattern of the binary complex SeMet BMP2(F41M,Y91M)–CV2 VWC1. The diffraction limit of these crystals was about 2.7 Å.

Y41M and F91M were chosen owing to their position outside the BMP type I and type II receptor-binding epitopes (Weber *et al.*, 2007). Interaction analysis using BIAcore showed that the binding affinity of BMP2(F41M,Y91M) to CV2 VWC1 is unaltered (data not shown). As an alternative approach, SeMet labelling of CV2 VWC1 was also planned. However, since the wild-type sequence of CV2 VWC1 lacks methionines and no structural data for CV2 VWC1 were available, four polar residues were selected for exchange to methionine. The single CV2 VWC1 mutants S28M, N33M, K39M and E41M could be expressed and purified in a similar manner as described for the wild-type protein. Their binding characteristics to BMP2 were analysed by BIAcore, showing that all mutants exhibited wild-type binding affinity (data not shown). Additionally, the CV2 VWC1 double mutants S28MN33M, N33ME41M and N33MK39M were prepared in order to further increase the number of methionines or to enable the use of unlabelled BMP2 in the complex; however, only the variant CV2 VWC1(N33M,K39M) could be prepared and isolated. The SeMet-labelled variants CV2 VWC1(N33M,K39M) and SeMet CV2 VWC1(S28M) were used for complex preparation with SeMet BMP2; however, only the complex SeMet BMP2–SeMet CV2 VWC1(S28M) yielded diffracting crystals.

The complexes SeMet BMP2(Y41M,F91M)–CV2 VWC1 and SeMet BMP2–SeMet CV2 VWC1(S28M) formed crystals similar to those of the wild-type proteins. For data acquisition, SeMet BMP2(Y41M,F91M)–CV2 VWC1 crystals were grown at 294 K from 2.0 *M* ammonium phosphate, 0.1 *M* Tris–HCl pH 7.5, 8%(*v*/*v*) glycerol, 5%(*w*/*v*) sucrose, whereas SeMet BMP2–SeMet CV2 VWC1(S28M) crystals were grown at 294 K from 2.2 *M* ammonium phosphate, 0.1 *M* Tris–HCl pH 7.5, 10%(*v*/*v*) glycerol. Crystallization experiments were performed at a protein concentration of 8 mg ml^{-1}. Crystals grew reproducibly within 10 d to approximate dimensions of 0.2 × 0.05 × 0.05 mm (Fig. 3). Three-wavelength data sets (inflection, peak and remote) were recorded from both crystals and processed using the software *HKL*-2000 (Otwinowski & Minor, 1997) and *CrystalClear* (Rigaku) (Table 2). Despite the fact that crystals of the two complexes grew under identical conditions, crystals of the complex SeMet BMP2(Y41M,F91M)–CV2 VWC1 belonged to space group $I4_1$, while crystals of the complex SeMet BMP2–SeMet CV2 VWC1(S28M) belonged to space group $P4_12_12$ (or $P4_32_12$). Trials to index the diffraction data of either SeMet BMP2(F41M,Y91M)–CV2 VWC1 or SeMet BMP2–SeMet CV2 VWC1(S28M) in the 'wrong' space group failed, showing that two clear crystal forms exist despite the almost identical unit-cell parameters (Table 3). Analysis of the data using the software *SHARP*/*autoSHARP* (Vonrhein *et al.*, 2007) showed the presence of seven out of eight Se sites in the asymmetric unit for crystals of the complex SeMet BMP2(Y41M,F91M)–CV2 VWC1 and six out of six Se sites for crystals of the complex SeMet BMP2–SeMet CV2 VWC1(S28M). In both cases almost all or all the expected Se positions were identified, confirming the presence of a binary complex consisting of a BMP2 dimer and two CV2 VWC1 domains in the asymmetric unit (Fig. 4), which is appropriate for a solvent content of around 63–65% (V_M = 3.3–3.6 Å^3 Da^{-1}; Matthews, 1968).

The structures of the mutant proteins are now being determined in order to determine the molecular basis of the formation of different space groups by the two complexes. The final structures of the complexes of CV2 VWC1 bound to BMP2 will provide the first insights into how BMP ligands are recognized by modulator proteins of the chordin family, of which CV2 is a member. It is possible that the unique function of VWC-containing BMP-modulator proteins in positively and negatively regulating BMP function will be deducible from the structural analysis. Knowing how the von Willebrand type C

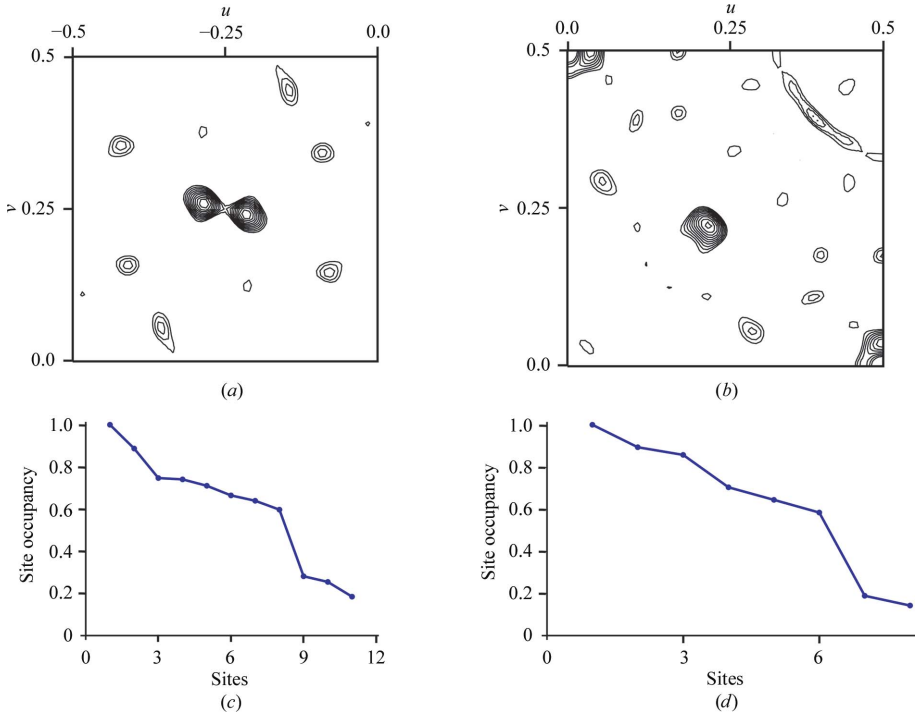

Figure 4
Harker sections of anomalous Pattersion maps of the complexes (*a*) BMP2(F41M,Y91M)–CV2 VWC1 (only z = 0.5 shown) and (*b*) BMP2–CV2 VWC1(S28M) (only z = 0.5 shown). The anomalous Patterson maps were produced with *CNS*, illustrating the data quality for phasing. *SHELXD* analysis of the data derived at peak wavelength suggest the presence of eight (*c*) and six (*d*) Se sites in the complexes BMP2(F41M,Y91M)–CV2 VWC1 and BMP2–CV2 VWC1(S28M), respectively, of which seven in BMP2(F41M,Y91M)–CV2 VWC1 and all six in BMP2–CV2 VWC1(S28M) could be refined with *SHARP*.

domain structurally interacts with cognate partners will also benefit the understanding of other protein–protein interactions in which VWC domains are involved.

We thank C. Schulze-Briese and T. Tomizaki from the Swiss Light Source for assistance during data acquisition and for access to the synchrotron-radiation beamline X06SA at the Swiss Light Source (SLS), Switzerland. We also wish to acknowledge access to the beamline PX14.2 at BESSY (Protein Structure Factory), Germany and thank H. Richter and M. Fuchs for their help during data acquisition. This project was supported by the Deutsche Forschungsgemeinschaft (DFG), MU1093/3-1.

References

Allendorph, G. P., Vale, W. W. & Choe, S. (2006). *Proc. Natl Acad. Sci. USA*, **103**, 7643–7648.
Binnerts, M. E., Wen, X., Cante-Barrett, K., Bright, J., Chen, H. T., Asundi, V., Sattari, P., Tang, T., Boyle, B., Funk, W. & Rupp, F. (2004). *Biochem. Biophys. Res. Commun.* **315**, 272–280.
Gazzerro, E. & Canalis, E. (2006). *Rev. Endocr. Metab. Disord.* **7**, 51–65.
Hogan, B. L. (1996). *Harvey Lect.* **92**, 83–98.
Ikeya, M., Kawada, M., Kiyonari, H., Sasai, N., Nakao, K., Furuta, Y. & Sasai, Y. (2006). *Development*, **133**, 4463–4473.
Jancarik, J. & Kim, S.-H. (1991). *J. Appl. Cryst.* **24**, 409–411.
Kirsch, T., Sebald, W. & Dreyer, M. K. (2000). *Nature Struct. Biol.* **7**, 492–496.
Kondo, M. (2007). *FEBS J.* **274**, 2960–2967.
Larrain, J., Bachiller, D., Lu, B., Agius, E., Piccolo, S. & De Robertis, E. M. (2000). *Development*, **127**, 821–830.
Larrain, J., Oelgeschlager, M., Ketpura, N. I., Reversade, B., Zakin, L. & De Robertis, E. M. (2001). *Development*, **128**, 4439–4447.
Li, X. & Cao, X. (2006). *Ann. NY Acad. Sci.* **1068**, 26–40.
McCoy, A. J., Grosse-Kunstleve, R. W., Adams, P. D., Winn, M. D., Storoni, L. C. & Read, R. J. (2007). *J. Appl. Cryst.* **40**, 658–674.
Matthews, B. W. (1968). *J. Mol. Biol.* **33**, 491–497.
O'Leary, J. M., Hamilton, J. M., Deane, C. M., Valeyev, N. V., Sandell, L. J. & Downing, A. K. (2004). *J. Biol. Chem.* **279**, 53857–53866.
Onichtchouk, D., Chen, Y. G., Dosch, R., Gawantka, V., Delius, H., Massague, J. & Niehrs, C. (1999). *Nature (London)*, **401**, 480–485.
Otwinowski, Z. & Minor, W. (1997). *Methods Enzymol.* **276**, 307–326.
Rentzsch, F., Zhang, J., Kramer, C., Sebald, W. & Hammerschmidt, M. (2006). *Development*, **133**, 801–811.
Ruppert, R., Hoffmann, E. & Sebald, W. (1996). *Eur. J. Biochem.* **237**, 295–302.
Samad, T. A., Rebbapragada, A., Bell, E., Zhang, Y., Sidis, Y., Jeong, S. J., Campagna, J. A., Perusini, S., Fabrizio, D. A., Schneyer, A. L., Lin, H. Y., Brivanlou, A. H., Attisano, L. & Woolf, C. J. (2005). *J. Biol. Chem.* **280**, 14122–14129.
Scheufler, C., Sebald, W. & Hulsmeyer, M. (1999). *J. Mol. Biol.* **287**, 103–115.
Simic, P. & Vukicevic, S. (2005). *Cytokine Growth Factor Rev.* **16**, 299–308.
Van Duyne, G. D., Standaert, R. F., Karplus, P. A., Schreiber, S. L. & Clardy, J. (1993). *J. Mol. Biol.* **229**, 105–124.
Vonrhein, C., Blanc, E., Roversi, P. & Bricogne, G. (2007). *Methods Mol. Biol.* **364**, 215–230.
Weber, D., Kotzsch, A., Nickel, J., Harth, S., Seher, A., Mueller, U., Sebald, W. & Mueller, T. D. (2007). *BMC Struct. Biol.* **7**, 6.
Zhang, J. L., Huang, Y., Qiu, L. Y., Nickel, J. & Sebald, W. (2007). *J. Biol. Chem.* **282**, 20002–20014.